Concomitant speed-of-sound tomography in photoacoustic imaging

Srirang Manohar[a)]
Biophysical Engineering Group, Faculty of Science and Technology, Institute for Biomedical Technology (BMTI), University of Twente, P.O. Box 217, 7500AE Enschede, The Netherlands

René G. H. Willemink, Ferdi van der Heijden, and Cornelis H. Slump
Signals and Systems Group, Faculty of Electrical Engineering, Mathematics and Computer Science, Institute for Biomedical Technology (BMTI), University of Twente, P.O. Box 217, 7500AE Enschede, The Netherlands

Ton G. van Leeuwen
Biophysical Engineering Group, Faculty of Science and Technology, Institute for Biomedical Technology (BMTI), University of Twente, P.O. Box 217, 7500AE Enschede, The Netherlands

(Received 29 April 2007; accepted 4 September 2007; published online 28 September 2007)

We present a method to generate quantitative cross-sectional maps of acoustic propagation speed in tissue using the photoacoustic principle. The method is based on the interaction of laser-induced ultrasound from an extraneous absorber with the object under photoacoustic investigation. The propagation times of the ultrasound transients through the object at angles around 360° are measured using a multielement ultrasound detector. The geometry lends itself to fan-beam reconstruction allowing speed-of-sound tomograms to be generated. Simultaneously, conventional photoacoustic computed tomography can be performed as well. We demonstrate the concept showing results on phantoms carrying speed-of-sound distributions. © *2007 American Institute of Physics*.
[DOI: 10.1063/1.2789689]

Photoacoustic (PA) imaging is quickly developing into a valuable modality for the three-dimensional visualization of physiology and pathology of soft tissue based on optical absorption contrast.[1] Photoacoustics is concerned with the nonradiative de-excitation of absorbed pulsed optical energy, where localized temperature rise results in the generation of ultrasound pulses due to the thermoelastic mechanism. These pulses propagate through soft tissue to be detected by a plurality of ultrasound detectors at the surface of the tissue. By applying various image reconstruction schemes, the location and strength of the internal ultrasound sources which are the optical absorbing structures can be determined. The technique is attractive since it allows depiction of absorbing structures in tissue with higher resolutions than purely optical imaging due to two to three orders of lower scattering experienced by ultrasound compared with light.

Reconstruction schemes employ as the "back-end," the backprojection of processed time-of-flight signal traces from each detection position into image space. Unlike in conventional x-ray computed tomography (CT) where backprojection is performed along straight lines, in photoacoustics backprojection is along concentric circular or spherical arcs.[2,3] In essence, an acoustic propagation speed is assumed for the medium in which the acoustic pulses propagate, allowing the time-axis of a measured signal trace to be converted into an equivalent distance axis, and the projection smeared out to generate a family of circular/spherical line integrals. Performing this "acoustic backprojection"[4] with appropriate filtering operations over all projections around the object, coherent summing builds up an image of photoacoustic sources. Two assumptions inherent to reconstruction schemes are that (1) the propagation speed-of-sound is known and (2) this is constant in the region of interest. In general, these assumptions are invalid in tissue. In most cases, the speed-of-sound (SOS) in the tissue is not measured; rather a typical value is chosen from the literature. Also, a single SOS is chosen for the entire object contrary to the knowledge that the parameter varies accending to tissue type and that the tissue under investigation may have a spatial distribution of SOS. The result of these assumptions is that there is no guarantee that acoustic backprojections will overlap, which could lead to compromised resolution and contrast.

There is a necessity to measure the spatial distribution of SOS to generate iso-delay backprojection paths. Further, acoustic propagation speed can be used to make images of tissue and disease state, and it has a diagnostic value in itself. While two methods have recently been proposed to measure SOS in the context of photoacoustics, both can be improved. The method of Kolkman *et al.*[5] requires the presence of well-defined absorbers in tissue which, in general, is not the case. The method of Jin and Wang[6] requires a separate ultrasound transmitter and necessitates extra measurements.

Our proposal permits SOS imaging in a photoacoustic imager based on a CT geometry, with minimum expense and without the requirement for additional measurements to the conventional PA protocol. The only hardware appendage is an absorber with a small cross section that is placed in the path of the laser light illuminating the object under photoacoustic examination. Figure 1(a) shows the schematic of the method with the absorber being a carbon fiber and the detector being a multielement array arranged antipodally with respect to the subject in water. Ultrasound transients are generated in the extraneous absorber and in the object by the photoacoustic effect. The carbon fiber ensures that the acoustic waves fan out in the imaging plane but are collimated in the direction orthogonal to this plane. The otherwise circular wavefront is distorted as the wave interacts with the object;

[a)]Electronic mail: S.Manohar@utwente.nl

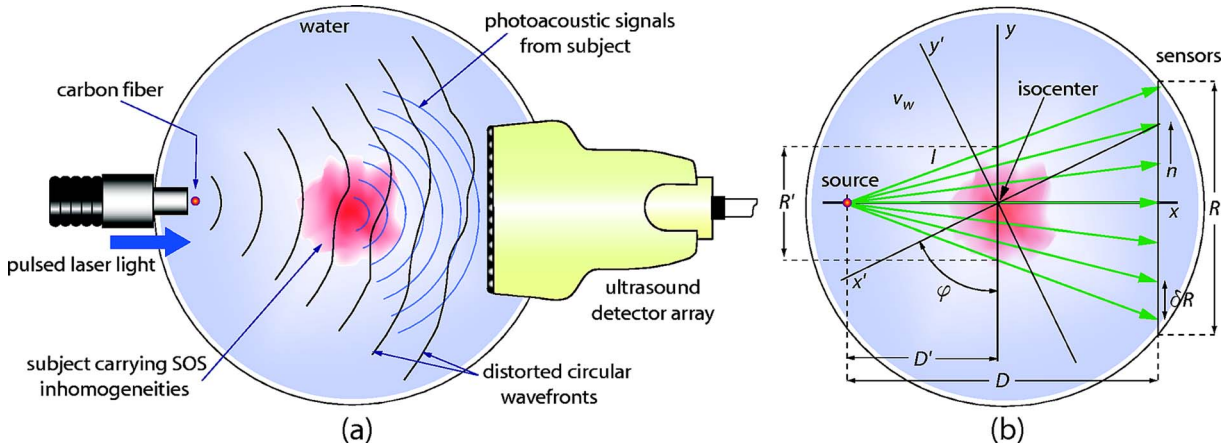

FIG. 1. (Color online) (a) A schematic of the method to measure speed-of-sound (SOS) cross-sectional images in a photoacoustic imager. Ultrasound transients are generated in the absorbing carbon fiber placed in the path of light illuminating the sample. The time-of-arrival (TOA) of the ultrasound transient is measured at each element of the ultrasound detector array. The photoacoustic signals from the object can be measured as well. (b) The TOA of the ultrasound transient at an individual element results from SOS variations along the ray from the source to the detector. This describes a fan-beam geometry which allows reconstruction enabling TOA and equivalently SOS tomography.

advancement (retardation) of the wavefront where regions of higher (lower) acoustic velocity are encountered. The wave propagates through the object to be collected at the far end by the individual elements of the ultrasound detector. The ultrasound detector measures conventional photoacoustic signals from the object as well; the two sets of signals have different times-of-arrival (TOAs) and are separated in the output trace of an element due to the finite distance between the carbon fiber and object. A calibration measurement is then made by retracting the object, allowing the ultrasound to propagate in water alone. In such a case, undistorted circular wavefronts can be expected.

Since the photoacoustic transient from the carbon fiber is broadband,[1] frequency dependent attenuation in tissue and the resulting dispersion could cause degeneration of the pulse shape through the object resulting in a loss of correlation with the calibration measurement pulse. In such a case, the standard cross-correlation operation[6] to ascertain time-delay differences between the object and calibration measurements could be unsuitable. We use instead the phase spectral difference[7] evaluated at a certain frequency f between the Fourier-analyzed pulses. A rough estimate of the TOA, obtained via cross-correlation, is used to set a window on the received signal within which the Fast Fourier Transform (FFT) is calculated. The phase difference between the windowed signal and calibration measurement signal is then used to calculate a correction delay,

$$\Delta t = \frac{\psi_w - \psi}{2\pi f}, \tag{1}$$

where ψ_w and ψ are the phase values at a specific frequency f of the Fourier transformed signals of the calibration and object measurements, respectively. The final TOA estimate is obtained by adding the correction delay to the rough TOA estimate. In a first approximation, the TOA of the ultrasound transient at a detector element is the line integral of the inverse of the SOS (Ref. 8) distribution encountered by a ray traversing the path from the source to the detector. The normalized TOA at element n is

$$t_\phi(n) = \int_{l(\phi,n)} \frac{ds}{v} - \int_{l(\phi,n)} \frac{ds}{v_w}, \tag{2}$$

where, with reference to Fig. 1(b), l is the ray path defined by rotation angle ϕ and detector position n, and v_w and v, are the phase velocities (Ref. 9) in water and object, respectively. The geometry in Fig. 1(b) can be recognized as the fan-beam projection geometry well-known from x-ray CT.

The hypothesis was tested on phantom measurements using a photoacoustic imager. The phantom is a SOS phantom without any optical absorbers. It is a cylinder of 3% agarose gel of 26 mm diameter, possessing 2 cavities of square cross-section with 8 and 5 mm sides as shown in Fig. 2(a). These cavities were filled with olive oil and then sealed. The phantom was mounted on a stepper motor driven rotary stage to be suspended in the center of an imaging tank. A carbon fiber of 250 μm diameter and 30 mm length is mounted vertically in the tank in the path of a laser beam of 18 mm diameter from a Q-switched Nd doped yttrium aluminum garnet laser emitting 5 ns pulses at 1064 nm. At the opposite side, a 128 element ultrasound detector array with a central frequency of 5 MHz is mounted through an aperture in the wall of the imaging tank. The signals from the array are multiplexed by a 128:4 MUX and acquired, using a quad-channel PCI digitizer (DC265, Acqiris, Geneva, Switzerland) triggered by a photodiode to sample at 100 MS/s. The imaging tank was filled with water maintained at 22 °C. A CT type measurement was performed with signals recorded from each element in 60 steps around the phantom. A single projection calibration experiment was performed with the phantom removed.

The measured TOA from the calibration experiment was fitted in a least squares sense to the model relating the geometry of the fan beam to the predicted TOA,

$$t(n) = \frac{\sqrt{D^2 + (n\,\delta R)^2}}{v_w}, \tag{3}$$

where, with reference to Fig. 1(b), D is the source-detector distance along the midline and δR is the detector element center-center spacing. This allows estimation of v_w (Ref. 9) used further to obtain the SOS tomogram.

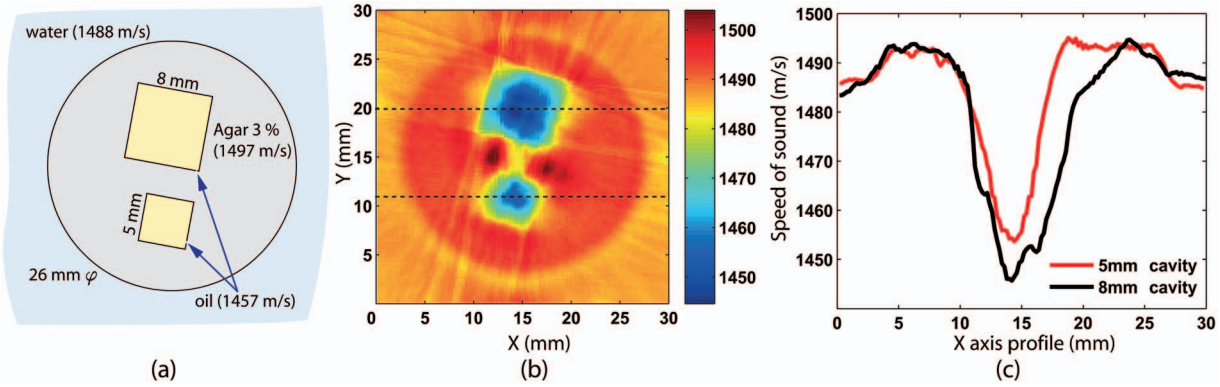

FIG. 2. (Color) (a) A schematic of the agar phantom surrounded by water with two square cross-sectional cavities filled with olive oil. (b) Speed-of-sound (SOS) tomogram of the phantom demonstrating the ability of the method to reconstruct SOS variations. The black dotted lines indicate the coordinates at which (c) intensity profiles are plotted.

First, the spatial distribution of ultrasound time delays per pixel needs to be estimated from the normalized TOAs [Eq. (1)] at 5 MHz. This delay map is represented by a set of triangular basis functions[10] with corresponding coefficients. A linear relation between the unknown coefficients and the obtained TOA sinogram values is then obtained by ray tracing along the integration paths defined in Eq. (2). The resulting linear system of equations is combined with a smoothness constraint on the gradient of the delay map to regularize the solution. The solution of the combined linear system is found with the iterative least-squares QR method[11] for large sparse matrices. The equivalent SOS tomogram can be inferred from the delay map using Eq. (2) with the estimated parameters from Eq. (3).

Figure 2(b) is the tomographic reconstruction of the phantom with horizontal lines marking the position of intensity profiles plotted in Fig. 2(c). It is seen that the two oil-filled cavities are clearly identified and the reconstructed SOS values in the image match independently measured values. Streaking artifacts at the edges of the oil cavities are present, which may be attributed to the refraction of the ultrasound beam, since sampling view requirements[12] for fan-beam CT have been fulfilled. This is possibly also the reason for the lower values imaged in the interior of the oil-filled cavities.

The spatial resolution depends on the dimensions of the detection element and the magnification $M=D/D'$ in Fig. 1(b). With the experimental parameters $D=89$ mm, $D'=59$ mm, element center-center spacing $\delta R=315$ μm, and element elevation height $h=4$ mm, the imaging plane resolution $(\delta R/M)$ and the elevation plane resolution (h/M) at the isocenter are, respectively, 0.208 and 2.65 mm.

We have demonstrated that speed-of-sound tomograms of a phantom can be generated in a conventional photoacoustic CT imager by using laser-induced ultrasound from an absorber to probe the object in the manner of ultrasound transmission CT. The technique facilitates hybrid SOS-photoacoustic imaging since the absorber has a small cross section so that a major portion of the incident light illuminates the object allowing conventional photoacoustic CT to be performed as well. We believe that hybrid SOS-PA CT has the potential for small-animal imaging and human breast imaging.

Assistance with instrumentation by Johan van Hespen is acknowledged. This research is funded by a personal grant to one of the authors (S.M.) in the Vernieuwingsimpuls program (TTF.6527) by the Netherlands Organisation of Scientific Research (NWO) and the Technology Foundation (STW). Authors acknowledge the Institute for Biomedical Technology (BMTI) of the University of Twente for funding in the NIMTIK program.

[1]M. Xu and L. V. Wang, Rev. Sci. Instrum. **77**, 04110 (2006).
[2]X. Wang, Y. Pang, G. Ku, X. Xie, G. Stoica, and L.-H. Wang, Nat. Biotechnol. **21**, 803 (2003).
[3]R. A. Kruger, W. L. Kiser, Jr., D. R. Reinecke, G. A. Kruger, and K. D. Miller, Mol. Imaging **2**, 113 (2003).
[4]S. J. Norton and M. Linzer, Ultrason. Imaging **1**, 154 (1979).
[5]R. G. M. Kolkman, W. Steenbergen, and T. G. van Leeuwen, Opt. Express **15**, 3291 (2007).
[6]X. Jin and L.-V. Wang, Phys. Med. Biol. **51**, 6437 (2006).
[7]W. Sachse and Y.-H. Pao, J. Appl. Phys. **49**, 4320 (1978).
[8]We use the term speed-of-sound as being synonymous to phase velocity in this letter.
[9]Since water is dispersionless, the group velocity and phase velocity are the same.
[10]K. M. Hanson and G. W. Wecksung, Appl. Opt. **24**, 23 (1985).
[11]C. C. Paige and M. A. Saunders, ACM Trans. Math. Softw. **8**, 1 (1982).
[12]P. M. Joseph and R. A. Schulz, Med. Phys. **7**, 692 (1980).